

Supplemental Material for Multifractional Brownian motion with telegraphic, stochastically varying exponent

Michał Balcerek,¹ Samudrajit Thapa,^{2,3,*} Krzysztof Burnecki,¹ Holger Kantz,² Ralf Metzler,⁴ Agnieszka Wyłomańska,¹ and Aleksei Chechkin^{1,4,5,6}

¹*Faculty of Pure and Applied Mathematics, Hugo Steinhaus Center, Wrocław University of Science and Technology, Wybrzeże Wyspiańskiego 27, 50-370 Wrocław, Poland*

²*Max Planck Institute for the Physics of Complex Systems, Noethnitzer Straße 38, 01187 Dresden, Germany*

³*Department of Physics, Indian Institute of Technology Guwahati, Guwahati 781039, Assam, India*

⁴*Institute of Physics & Astronomy, University of Potsdam, 14476 Potsdam, Germany*

⁵*German-Ukrainian Core of Excellence, Max Planck Institute of Microstructure Physics, Weinberg 2, 06120 Halle, Germany*

⁶*Akhiezer Institute for Theoretical Physics, National Science Center 'Kharkiv Institute of Physics and Technology', Akademichna st.1, Kharkiv 61108, Ukraine*

(Dated: April 17, 2025)

I. Derivation of the ACVF Eq. (2)

Let us start with the spectral representation of FBM given by Eq. (1) in the main text with $\mathcal{H}(t) = H = \text{constant}$. The MSD is then given as

$$\begin{aligned} \langle B_H^2(t) \rangle &= C^2(H) \int_{-\infty}^{\infty} \frac{(e^{i\omega t} - 1)(e^{-i\omega t} - 1)}{|\omega|^{2H+1}} d\omega = 4C^2(H) \int_0^{\infty} \frac{1 - \cos \omega t}{\omega^{2H+1}} d\omega \\ &= \frac{\pi}{H\Gamma(2H) \sin(\pi H)} C^2(H) t^{2H} = \frac{2\pi}{\Gamma(2H+1) \sin(\pi H)} C^2(H) t^{2H}. \end{aligned} \quad (1)$$

Thus, imposing $\langle B_H^2(t) \rangle = t^{2H}$ gives the expression for $C(H)$ as

$$C(H) = \sqrt{\frac{\Gamma(2H+1) \sin(\pi H)}{2\pi}}. \quad (2)$$

The autocovariance function (ACVF) for FBM calculated from the spectral representation thus takes the form

$$\langle B_H(t_1) B_H(t_2) \rangle = C^2(H) \int_{-\infty}^{\infty} \frac{(e^{i\omega t_1} - 1)(e^{-i\omega t_2} - 1)}{|\omega|^{2H+1}} d\omega = \frac{1}{2} [t_1^{2H} + t_2^{2H} - |t_2 - t_1|^{2H}]. \quad (3)$$

Let us consider Eq. (1) of the main text and calculate the ACVF conditional on $\mathcal{H}(t)$:

$$\langle B_{\mathcal{H}(t_1)}(t_1) B_{\mathcal{H}(t_2)}(t_2) \rangle = C(\mathcal{H}(t_1)) C(\mathcal{H}(t_2)) \int_{-\infty}^{\infty} \frac{(e^{i\omega t_1} - 1)(e^{-i\omega t_2} - 1)}{|\omega|^{\mathcal{H}(t_1)+\mathcal{H}(t_2)+1}} d\omega. \quad (4)$$

Now let's fix t_1 and t_2 , and introduce $H = (\mathcal{H}(t_1) + \mathcal{H}(t_2))/2$. Then we can write (see Eq. (3))

$$\begin{aligned} \int_{-\infty}^{\infty} \frac{(e^{i\omega t_1} - 1)(e^{-i\omega t_2} - 1)}{|\omega|^{\mathcal{H}(t_1)+\mathcal{H}(t_2)+1}} d\omega &= \frac{1}{C^2(H)} \langle B_H(t_1) B_H(t_2) \rangle \\ &= \frac{1}{2C^2(H)} [t_1^{2H} + t_2^{2H} - |t_2 - t_1|^{2H}], \end{aligned} \quad (5)$$

where $C(H)$ is given by Eq. (2). After plugging Eq. (5) into Eq. (4) we get

$$\begin{aligned} \langle B_{\mathcal{H}(t_1)}(t_1) B_{\mathcal{H}(t_2)}(t_2) \rangle &= \frac{C(\mathcal{H}(t_1)) C(\mathcal{H}(t_2))}{2C^2(H)} \\ &\times \left[t_1^{\mathcal{H}(t_1)+\mathcal{H}(t_2)} + t_2^{\mathcal{H}(t_1)+\mathcal{H}(t_2)} - |t_2 - t_1|^{\mathcal{H}(t_1)+\mathcal{H}(t_2)} \right]. \end{aligned} \quad (6)$$

Thus we arrive at Eq. (2) in the main text.

* thapa@pks.mpg.de

II. Beta distribution as the stationary PDF for smoothed telegraph process

Let us obtain the stationary PDF of the process governed by the Langevin equation

$$\frac{dx}{dt} = f(x) + \xi(t), \quad (7)$$

where f is a deterministic function and $\xi(t)$ is a telegraph process, i.e. a stationary dichotomic Markov process that jumps between two values c_1 and c_2 , $c_1 < c_2$, with mean rates $\lambda(c_1 \rightarrow c_2) = \lambda_{12}$ and $\lambda(c_2 \rightarrow c_1) = \lambda_{21}$. The mean and the ACVF of ξ are given respectively by

$$\langle \xi \rangle = \frac{1}{2\lambda} (\lambda_{12}c_2 + \lambda_{21}c_1) \quad (8)$$

and

$$\langle \xi(t)\xi(t') \rangle = \langle \xi \rangle^2 + \frac{\lambda_{12}\lambda_{21}(c_2 - c_1)^2}{4\lambda^2} \exp(-2\lambda|t - t'|), \quad (9)$$

where $\lambda = (\lambda_{12} + \lambda_{21})/2$.

Here we employ the approach and notations used in [1]. Let's introduce the "microscopic density",

$$\rho(x, t) = \delta(x - x(t)), \quad (10)$$

which obeys the equation

$$\frac{\partial \rho}{\partial t} + \frac{\partial}{\partial x} [(f(x) + \xi(t))\rho] = 0. \quad (11)$$

Introducing $p(x, t) = \langle \delta(x - x(t)) \rangle$ and averaging Eq. (11) one gets

$$\frac{\partial p}{\partial t} + \frac{\partial}{\partial x} (f(x)p) + \frac{\partial p_1}{\partial x} = 0, \quad (12)$$

where $p_1(x, t) = \langle \xi(t)\rho \rangle$. Following [1] and using the "formula of differentiation" [2], we arrive at

$$\frac{\partial p_1}{\partial t} = -2\lambda p_1 - \frac{\partial}{\partial x} [f(x)p_1] - (c_1 + c_2) \frac{\partial p_1}{\partial x} + c_1 c_2 \frac{\partial p}{\partial x} + (\lambda_{12}c_2 + \lambda_{21}c_1)p. \quad (13)$$

Now we consider $f(x) = -\gamma x$ where γ is constant, and after some transformations of Eqs. (12) and (13) we arrive at the following closed equation for p

$$\begin{aligned} \frac{\partial^2 p}{\partial t^2} + (2\lambda - 3\gamma) \frac{\partial p}{\partial t} + (c_1 + c_2 - 2\gamma x) \frac{\partial^2 p}{\partial x \partial t} + [\gamma^2 x^2 + c_1 c_2 - \gamma x(c_1 + c_2)] \frac{\partial^2 p}{\partial x^2} \\ + [4\gamma^2 x - 2\lambda\gamma x - 2\gamma(c_1 + c_2) + \lambda_{12}c_2 + \lambda_{21}c_1] \frac{\partial p}{\partial x} + 2\gamma(\gamma - \lambda)p = 0. \end{aligned} \quad (14)$$

We are looking for the stationary solution of Eq. (14). Putting $\frac{\partial p}{\partial t} = 0$, and then integrating with respect to x we obtain the particular solution as

$$p(x) = \mathcal{N} \left(x - \frac{c_1}{\gamma} \right)^{\frac{\lambda_{12}}{\gamma} - 1} \left(\frac{c_2}{\gamma} - x \right)^{\frac{\lambda_{21}}{\gamma} - 1}, \quad \frac{c_1}{\gamma} < x < \frac{c_2}{\gamma}, \quad (15)$$

where \mathcal{N} is the normalization constant. To go back to our notations in the main text, we change $c_{1,2}/\gamma \rightarrow H_{1,2}$, $\gamma \rightarrow \tau^{-1}$ and arrive at the beta distribution presented in Eq. (6) of the main text.

Fig. 1 shows how the flexibility of beta distribution can be leveraged to realize different shapes depending on the choice of parameters.

III. Derivation of the ACVF of smoothed telegraph process

A simple derivation of Eqs. (7) and (8) in the main text is specified in [3]. Because of stationarity, $\langle \mathcal{H}(t) \rangle = \langle \mathcal{H}_{TP}(t) \rangle$, and in notations of [3] it is given by

$$\mu_{x1} = q_0 a_0 + q_1 a_1, \quad (16)$$

while ACVF is given by Eq.(12) in [3]. To establish the correspondence with Eq. (8) in the main text, one changes

$$q_0 = \nu_1/\nu \rightarrow \lambda_{21}/(2\lambda), \quad q_1 = \nu_0/\nu \rightarrow \lambda_{12}/(2\lambda), \quad a_0 \rightarrow H_1, \quad a_1 \rightarrow H_2. \quad (17)$$

IV. Alternative models of $\mathcal{H}(t)$

The Ornstein-Uhlenbeck process (OUP) given as a stationary solution of the stochastic differential equation

$$dX_t = \theta(\mu - X_t)dt + \sigma dB_t \quad (18)$$

and the square of the OUP are good alternatives to model $\mathcal{H}(t)$. Similarly to the smoothed telegraph process, they can model the time-varying nature of $\mathcal{H}(t)$, with the advantage of being mean-reverting and having well-understood stochastic properties. On top of that, we know that the OUP is a continuous-time Gaussian process with an exponentially decaying autocorrelation function. When squared, it provides non-negative values important for considering the range of $\mathcal{H}(t)$. Naturally, such models have to be treated with greater care than the smoothed telegraph process, since their possible values span all reals (for OUP) and non-negative reals (for its square). One alternative is to utilize the OUP reflected at the origin [4–6].

In Fig. 2 we present the behavior of sample realizations of $\mathcal{H}(t)$, where the left panel corresponds to the OUP with parameters $\theta = 0.08, \mu = 0.5, \sigma = 0.06$ and time-step 0.01, and the right panel corresponds to its square. In Fig. 3 we present trajectories of MBM that correspond to the chosen model of $\mathcal{H}(t)$ – the left panel utilizes the OUP model for $\mathcal{H}(t)$, the right panel corresponds to its square. In Fig. 4 we show sample ACVFs as functions of lag time Δ for the estimated Hurst exponents of the two processes considered here. They both exhibit an exponential-like decay similarly to the ACVF of the smoothed telegraph process.

V. Simulation algorithm

In this part we describe in details the simulation algorithm for **telegraphic multifractional Brownian motion** $B_{\mathcal{H}}(t)$ in times $t_1 < t_2 < \dots < t_n$. For the sake of simplicity let's consider equally spaced t_k 's, i.e. $t_k = k \cdot \Delta, k = 1, 2, \dots, n$. Then the algorithm to simulate TeMBM is as follows:

1. Simulate the trajectory of the process $\mathcal{H}(t)$ in times t_1, t_2, \dots, t_n . The algorithm depends on the type of the process. Below we present how to simulate the sample trajectory of the smoothed telegraph process.
2. Given $\mathcal{H}(t_k)$ for $k = 1, 2, \dots, n$ construct the autocovariance matrix of vector $[B_{\mathcal{H}}(t_1), B_{\mathcal{H}}(t_2), \dots, B_{\mathcal{H}}(t_n)]'$, that is

$$\Sigma = [\langle B_{\mathcal{H}}(t_i) B_{\mathcal{H}}(t_j) \rangle]_{1 \leq i, j \leq n},$$

where $\langle B_{\mathcal{H}}(t_i) B_{\mathcal{H}}(t_j) \rangle$ is the ACVF of the MBM given in Eq. (2) in the main text.

3. Use Cholesky algorithm, i.e. decompose matrix Σ to find the lower triangular matrix L , and then

$$\begin{bmatrix} B_{\mathcal{H}}(t_1) \\ B_{\mathcal{H}}(t_2) \\ \vdots \\ B_{\mathcal{H}}(t_n) \end{bmatrix} = L \cdot \begin{bmatrix} Z_1 \\ Z_2 \\ \vdots \\ Z_n \end{bmatrix}$$

where Z_1, Z_2, \dots, Z_n are independent identically distributed standard normal random variables. For example, it can be done using a built-in function `chol`(Σ , 'lower') in Matlab; `np.linalg.cholesky`(Σ) in Python using `numpy` library; or `cholesky`(Σ).L from `LinearAlgebra` library in Julia.

Simulation algorithm for **smoothed telegraph process** $\mathcal{H}(t)$ in times $t_1 < t_2 < \dots < t_n$ is as follows:

1. First, generate telegraph process $\mathcal{H}_{TP}(t)$ in the same times t_1, t_2, \dots, t_n :
 - (a) Set current state `state = rand(0,1)`, i.e. a random number 0 or 1. If a stationary version of the telegraph process is required, choose 0 with probability $\frac{\lambda_{12}}{\lambda_{12} + \lambda_{21}}$, and 1 with probability $\frac{\lambda_{21}}{\lambda_{12} + \lambda_{21}}$.
 - (b) Set `ind = 1`
 - (c) If `state == 0` then set `len = [rand(\mathcal{E}_0)]`, a random number from exponential distribution with rate $\Delta \cdot \lambda_{12}$, otherwise `len = [rand(\mathcal{E}_1)]`, a random number from exponential distribution with rate $\Delta \cdot \lambda_{21}$.
 - (d) Set $\mathcal{H}_{TP}(t_{\text{ind}}), \mathcal{H}_{TP}(t_{\text{ind}+1}), \dots, \mathcal{H}_{TP}(t_{\text{ind}+\text{len}-1})$ to `state`.
 - (e) `state = 1 - state`

- (f) $\text{ind} = \text{ind} + \text{len}$
- (g) If $\text{ind} < n$ then go back to (c).
- (h) Rescale the values of \mathcal{H}_{TP} to H_1 and H_2 instead of 0 and 1: $\mathcal{H}_{TP}(t_k) = \mathcal{H}_{TP}(t_k) \cdot (H_2 - H_1) + H_1$ for $k = 1, 2, \dots, n$.

2. To obtain smoothed telegraph process:

- (a) Set $\mathcal{H}(t_1) = \text{rand}(\mathcal{B})$, a random number from stationary STP distribution given by beta distribution in Eq. (4) in the main text.
- (b) For $k = 2, 3, \dots, n - 1$ set $\mathcal{H}(t_{k+1}) = \mathcal{H}(t_k) + \Delta \cdot \frac{\mathcal{H}_{TP}(t_k) - \mathcal{H}(t_k)}{\tau}$.

VI. Estimation algorithm

Let us consider M random samples of length N

$$\mathbb{X}_N^i = \{X^i(t_1), X^i(t_2), \dots, X^i(t_N)\}, \quad i = 1, 2, \dots, M. \quad (19)$$

The estimation algorithm for the Hurst exponent is as follows:

1. We select a segment length w and an overlapping length o .
2. Each sample trajectory \mathbb{X}_N^i , $i = 1, 2, \dots, M$ is divided into segments of length w with the overlapping length of o points. We denote them as $\mathbb{X}_N^{i,1}, \mathbb{X}_N^{i,2}, \dots, \mathbb{X}_N^{i,m}$, where m is the total number of segments constructed from the i -th trajectory.
3. For each segment $\mathbb{X}_N^{i,j}$ we use TAMS-based approach to estimate the Hurst exponent. The estimated values are denoted as $H^{i,j}$, $i = 1, 2, \dots, M$, $j = 1, 2, \dots, m$.

VII. Distinguishing algorithm

We consider M random samples of length N , see Eq. (19) for the notation. To discern whether the sample trajectories correspond to FBM, FBMRE or TeMBM we proceed as follows:

1. For each sample trajectory \mathbb{X}_N^i , $i = 1, 2, \dots, M$ we estimate the Hurst exponents $H^{i,j}$, $i = 1, 2, \dots, M$, $j = 1, 2, \dots, m$, according to the estimation algorithm presented above.
2. For each $j, k = 1, 2, \dots, m$ we estimate the sample ACVF

$$\gamma(j, k) = \sum_{i=1}^M \left(H^{i,j} - \overline{H^j} \right) \left(H^{i,k} - \overline{H^k} \right), \quad (20)$$

where $\overline{H^j} = \frac{1}{M} \sum_{i=1}^M H^{i,j}$.

3. For fixed j we analyze the function $\gamma(j, k)$. More precisely, if for large values of k $\gamma(j, k)$ stabilizes at zero level, then the sample trajectories correspond to FBM. On the other hand, if $\gamma(j, k)$ stabilizes at some non-zero level, then the sample trajectories correspond to FBMRE. Finally, if we observe a decay of $\gamma(j, k)$, the sample trajectories can be attributed to TeMBM.

Let us note, that in the above-described distinguishing algorithm, we do not take into account the diffusion coefficient. This can be done only under certain conditions which we discuss here. The Hurst index H is estimated from the slope of the log-log plot of TAMS vs. Δ after selecting a window size, w . The diffusion-coefficient appears only as the y -intercept in the log-log plot, and therefore should not significantly effect the estimation of H . Fig. 2 in the main text shows that our estimates of H are reasonable and results in the same distribution as the original stationary distribution of H that underlay the generation of TeMBM trajectories.

The Python source code for the simulations and estimations is available on GitHub [7].

VIII. Description of the real-world datasets

Dataset 1: This dataset consists of the time series of mean daily temperature data, from 01.01.1955 to 31.12.2020, collected at 10 different meteorological stations in Germany [8, 9]. The stations were chosen such that there are no missing data points. Exact details of the stations are provided in the Table I. We consider the time series of temperature anomalies, namely, the deviations of the daily temperature at a given calendar day of the year from the average daily temperature at that particular calendar day, where the average is over all the years considered. It was shown previously that the time series of such temperature anomalies could be modelled with fractional Gaussian noise but with additional short range correlations of 4-5 days [10, 11]. In order to remove the short range correlations we take a weekly average of the temperature anomalies, and then take a cumulative sum to obtain FBM-like trajectories. Finally to create a larger ensemble of trajectories, we split each trajectory into 4 trajectories, so that our dataset consists of 40 trajectories, each with $N = 860$ data points.

TABLE I. Details of the meteorological stations from which the daily mean temperature data was taken to construct dataset 1.

Location	Latitude (degrees:minutes:seconds)	Longitude (degrees:minutes:seconds)	Height (meters)
Bamberg	+49:52:31	+010:55:18	240
Berlin-Dahlem	+52:27:50	+013:18:06	51
Bremen	+53:02:47	+008:47:57	4
Frankfurt	+50:02:47	+008:35:54	112
Hohenpeissenberg	+47:48:06	+011:00:42	977
Jena Sterwarte	+50:55:36	+011:35:03	155
Muenchen	+48:09:51	+011:32:39	515
Potsdam	+52:23:00	+013:03:50	81
Schwerin	+53:38:39	+011:23:18	59
Zugspitze	+47:25:19	+010:59:12	2964

Dataset 2: This dataset consists of 3834 trajectories—each with $N = 100$ data points measured with an experimental time resolution of 100 ms—corresponding to quantum dots tracked in the cytoplasm of mammalian cells [12]. It was shown previously that this dataset corresponds to FBMRE with the Hurst exponent beta distributed [13].

Dataset 3: This dataset consists of 532 trajectories—each with $N = 300$ data points measured with an experimental time resolution of 33 ms—corresponding to micron-sized beads tracked in mucin hydrogels at acidic conditions ($pH = 2$) and with zero salt concentration [14]. It was shown previously that this dataset too corresponds to FBMRE with the Hurst exponent beta distributed [13, 15].

Dataset 4: This dataset describes day ahead electricity price in the year 2022 from the bidding zone between Germany and Luxembourg (BZN—DE-LU). The data are quoted every 15 minutes and are publicly available on the web page [16]. In order to obtain an ensemble of trajectories we split the time series into 51 trajectories corresponding to week periods (Monday 00:00 – Sunday 23:45). Consequently, each trajectory has 672 observations.

IX. Additional results for electricity price data

In Fig. 5 we demonstrate the results for six different starting time points t used in the distinguishing procedure. The labels “Monday”, “Tuesday”, etc. mean that the starting point t in sample ACVF $\gamma(t, t + \Delta)$ calculation is the first observation (hour) on Monday, Tuesday, etc., respectively. All the cases are indicative of TeMBM.

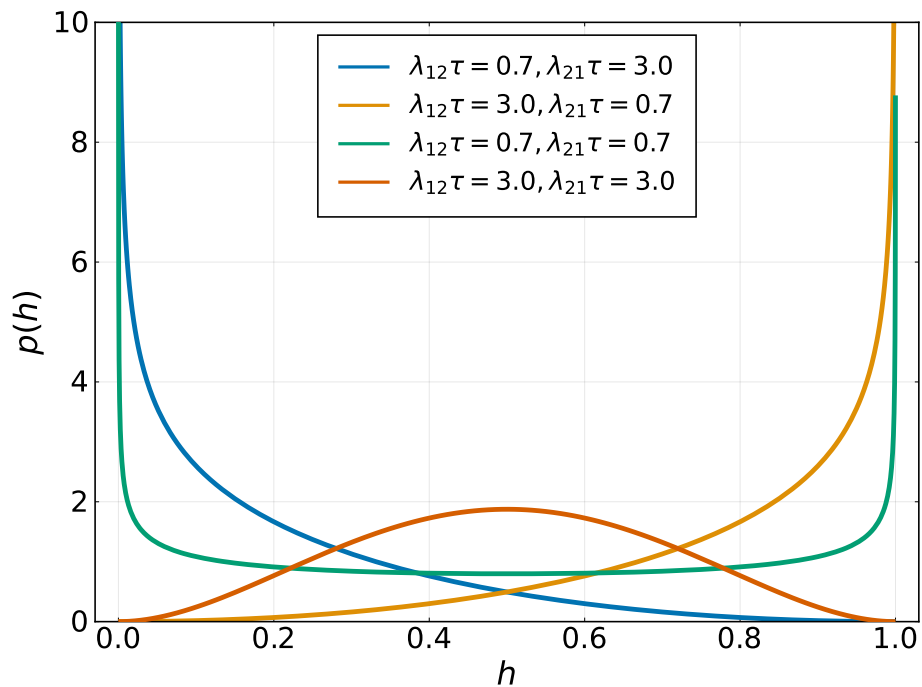


FIG. 1. Representative shapes of the beta distribution (Eq. (6) in the main text) highlights its flexibility via specific choice of parameters to potentially describe various experimental observations.

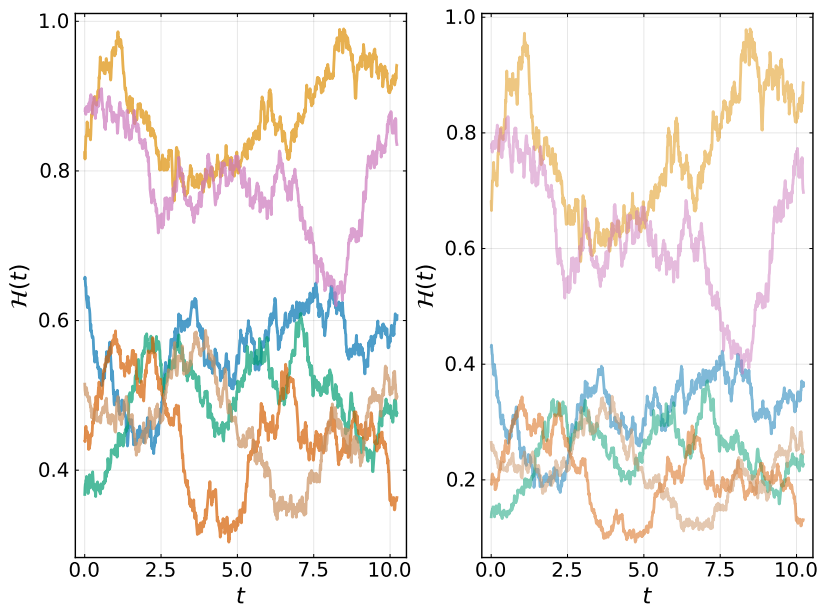


FIG. 2. Sample paths of the OUP with parameters $\theta = 0.08$, $\mu = 0.5$, $\sigma = 0.06$ (left panel) and its square (right panel).

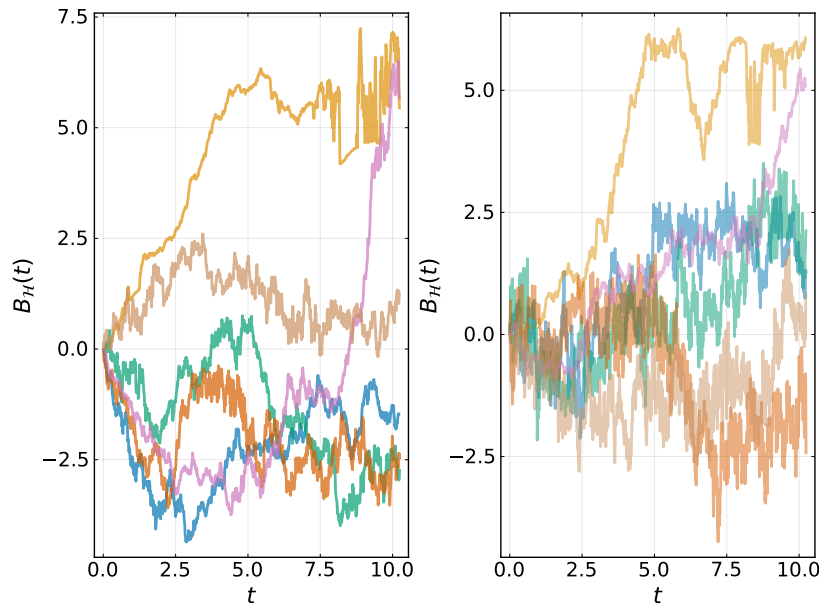


FIG. 3. Sample paths of MBM with $\mathcal{H}(t)$ modelled by the OUP (left panel) and by its square (right panel). The parameters of the OUP are the same as before, i.e., $\theta = 0.08, \mu = 0.5, \sigma = 0.06$.

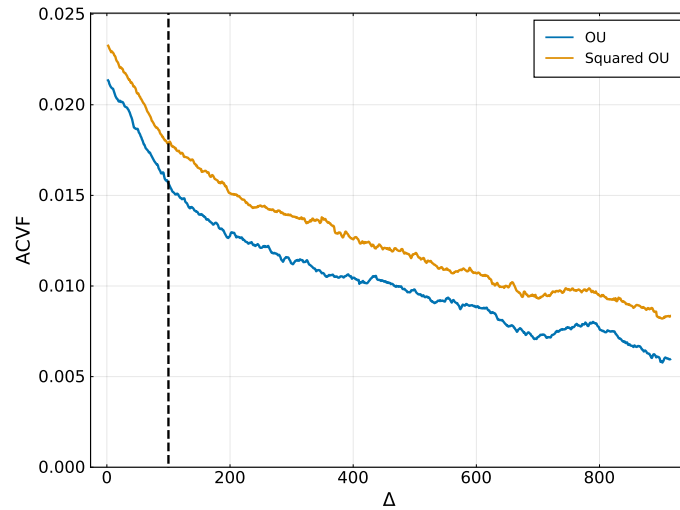


FIG. 4. Sample ACVFs as function of the lag time Δ for the estimated Hurst exponents from 5,000 trajectories of MBM with $\mathcal{H}(t)$ modelled by the OUP (“OU”) and by its square (“Squared OU”). The parameters of the OUP are the same as before, i.e., $\theta = 0.08, \mu = 0.5, \sigma = 0.06$.

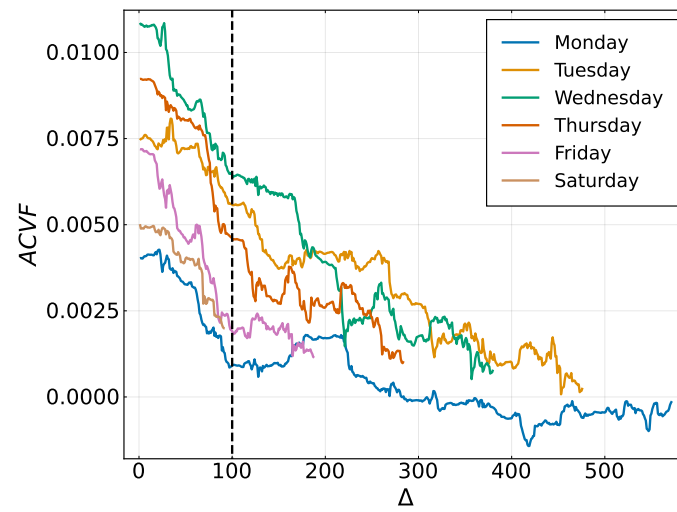


FIG. 5. Results of the process-distinguishing procedure for electricity price data for different starting points t . The labels “Monday”, “Tuesday”, etc. mean that the starting point t in sample ACVF $\gamma(t, t + \Delta)$ calculation is the first observation (hour) on Monday, Tuesday, etc., respectively.

-
- [1] J. M. Sancho, *J. Math. Phys.* **25**, 354 (1984).
 - [2] V. E. Shapiro and V. M. Loginov, *Phys. A: Stat. Mech. Appl.* **91**, 563 (1978).
 - [3] R. FitzHugh, *Mathematical Biosciences* **64**, 75 (1983).
 - [4] A. V. Skorokhod, *Theory of Probability & Its Applications* **6**, 264 (1961).
 - [5] V. Giorno, A. G. Nobile, and L. Ricciardi, *Advances in Applied Probability* **18**, 991 (1986).
 - [6] A. R. Ward and P. W. Glynn, *Queueing Systems* **43**, 103 (2003).
 - [7] M. Balcerek, “Python notebook including the simulation and estimation codes,” <https://github.com/MichalBalcerek/Multifractional-Brownian-motion-with-telegraphic-stochastically-varying-exponent> (2024).
 - [8] A. M. G. K. Tank, J. B. Wijngaard, G. P. Können, R. Böhm, G. Demarée, A. Gocheva, M. Mileta, S. Pashiardis, L. Hejkrlik, C. Kern-Hansen, R. Heino, P. Bessemoulin, G. Müller-Westermeier, M. Tzanakou, S. Szalai, T. Pálsdóttir, D. Fitzgerald, S. Rubin, M. Capaldo, M. Maugeri, A. Leitass, A. Bukantis, R. Aberfeld, A. F. V. van Engelen, E. Forland, M. Mietus, F. Coelho, C. Mares, V. Razuvaev, E. Nieplova, T. Cegnar, J. A. López, B. Dahlström, A. Moberg, W. Kirchhofer, A. Ceylan, O. Pachaliuk, L. V. Alexander, and P. Petrovic, *Int. J. Climatol.* **22**, 1441 (2002).
 - [9] “European Climate Assessment & Dataset project webpage,” <http://www.ecad.eu> (2024).
 - [10] M. Massah and H. Kantz, *Geophys. Res. Lett.* **43**, 9243 (2016).
 - [11] S. Thapa, A. Wyłomańska, G. Sikora, C. E. Wagner, D. Krapf, H. Kantz, A. V. Chechkin, and R. Metzler, *New J. Phys.* **23**, 013008 (2021).
 - [12] A. Sabri, X. Xu, D. Krapf, and M. Weiss, *Phys. Rev. Lett.* **125**, 058101 (2020).
 - [13] M. Balcerek, K. Burnecki, S. Thapa, A. Wyłomańska, and A. Chechkin, *Chaos: An Interdisciplinary Journal of Nonlinear Science* **32**, 093114 (2022).
 - [14] C. E. Wagner, B. S. Turner, M. Rubinstein, G. H. McKinley, and K. Ribbeck, *Biomacromolecules* **18**, 3654 (2017).
 - [15] A. G. Cherstvy, S. Thapa, C. E. Wagner, and R. Metzler, *Soft Matter* **15**, 2526 (2019).
 - [16] “ENTSO-E webpage,” entsoe.eu (2024).